processes

MDPI

Article

Anti-Inflammatory and Anti-Diabetic Activity of Ferruginan, a Natural Compound from *Olea ferruginea*

Abdur Rauf [1,*], Umer Rashid [2], Zafar Ali Shah [1], Gauhar Rehman [3], Kashif Bashir [4], Johar Jamil [5], Iftikhar [1], Abdur Rahman [3], Abdulrahman Alsahammari [6], Metab Alharbi [6], Abdulmajeed Al-Shahrani [7] and Giovanni Ribaudo [8,*]

1 Department of Chemistry, University of Swabi, Swabi, Anbar 23430, Pakistan
2 Department of Chemistry, COMSATS University Islamabad, Abbottabad Campus, Islamabad 22060, Pakistan
3 Department of Zoology, Abdul Wali Khan University, Mardan 23200, Pakistan
4 Department of Health and Biological Sciences, Abasyn University, Peshawar 25000, Pakistan
5 Department of Microbiology, University of Swabi, Swabi, Anbar 23430, Pakistan
6 Department of Pharmacology and Toxicology, College of Pharmacy, King Saud University, P.O. Box 2455, Riyadh 11451, Saudi Arabia
7 Laboratory Department, Almadah General Hospital, Ministry of Health, Riyadh 10336, Saudi Arabia
8 Dipartimento di Medicina Molecolare e Traslazionale, Università Degli Studi di Brescia, Viale Europa 11, 25123 Brescia, Italy
* Correspondence: abdurrauf@uoswabi.edu.pk (A.R.); giovanni.ribaudo@unibs.it (G.R.)

Abstract: Inflammation is a complex response of the human organism and relates to the onset of various disorders including diabetes. The current research work aimed at investigating the anti-inflammatory and anti-diabetic effects of ferruginan, a compound isolated from *Olea ferruginea*. Its in vitro anti-inflammatory activity was determined by using the heat-induced hemolysis assay, while the anti-diabetic effect of the compound was studied by the yeast cell glucose uptake assay. Ferruginan exhibited a maximum of 71.82% inhibition of inflammation and also increased the uptake of glucose by yeast cells by up to 74.96% at the highest tested concentration (100 µM). Moreover, ferruginan inhibited α-amylase dose-dependently, by up to 75.45% at the same concentration. These results indicated that ferruginan possesses promising anti-inflammatory and anti-diabetic properties in vitro, even if at high concentrations. To provide preliminary hypotheses on the potentially multi-target mechanisms underlying such effects, docking analyses were performed on α-amylase and on various molecular targets involved in inflammation such as 5′-adenosine monophosphate-activated protein kinase (AMPK, PDB ID 3AQV), cyclooxygenase (COX-1, PDB ID 1EQG, and COX-2, 1CX2), and tumor necrosis factor alpha (TNF-α, PDB ID 2AZ5). The docking studies suggested that the compound may act on α-amylase, COX-2, and AMPK.

Keywords: *Olea ferruginea*; *Oleaceae*; ferruginan; anti-inflammatory; anti-diabetic; molecular docking

check for updates

Citation: Rauf, A.; Rashid, U.; Shah, Z.A.; Rehman, G.; Bashir, K.; Jamil, J.; Iftikhar; Rahman, A.; Alsahammari, A.; Alharbi, M.; et al. Anti-Inflammatory and Anti-Diabetic Activity of Ferruginan, a Natural Compound from *Olea ferruginea*. *Processes* **2023**, *11*, 545. https://doi.org/10.3390/pr11020545

Academic Editors: Alina Bora and Luminita Crisan

Received: 19 January 2023
Revised: 7 February 2023
Accepted: 9 February 2023
Published: 10 February 2023

Copyright: © 2023 by the authors. Licensee MDPI, Basel, Switzerland. This article is an open access article distributed under the terms and conditions of the Creative Commons Attribution (CC BY) license (https://creativecommons.org/licenses/by/4.0/).

1. Introduction

Diabetes mellitus (DM) comprehends a group of metabolic diseases related to impaired insulin secretion, insensitivity of the target tissues to insulin, or a combination of these phenomena. The hallmark feature of DM is uncontrolled hyperglycemia, which causes severe complications. Additionally, the occurrence of diabetes is aggressively increasing worldwide, and this condition appears to be related to inflammation [1].

Natural products, especially those derived from plants, have been used for therapeutic applications towards several diseases from the ancient ages, and there are several examples of natural compounds being used or investigated as therapeutic agents also in more recent times [2–4]. In particular, *Olea* is a genus that comprehends forty common species belonging to the *Oleaceae* family. *Olea ferruginea* is one of the most widespread species of the *Olea* genus, which is found in Afghanistan, Pakistan, and Kashmir, as well as in the Mediterranean region [5].

A variety of compounds and preparations isolated from *Olea* plants have been traditionally used to treat various diseases, and native peoples use its stem bark to treat fevers. The bark and oil of this plant have been utilized to treat diabetes, headache, and asthma [5]. *O. ferruginea* also finds application as an antimalarial, anti-leprosy, and antitumor agent in traditional medicine, and the *O. ferruginea* fruit oil can treat arthritis and bone fractures [6]. More specifically, the fruits of *O. ferruginea* are a source of antioxidants, antidiabetic, and antihypertensive agents. Traditionally, *O. ferruginea* has shown antimalarial, anti-leprosy, and antitumor activity [6].

The *Olea* genus is a rich source of many natural compounds such as flavonoids and other phenolic substances including secoiridoid glycosides, lignans, and other compounds [7]. Secoiridoid and triterpenoids were previously identified in *O. ferruginea*, and their cytotoxic and alkaline phosphatase inhibitory activities were studied. A flavanone and a secoiridoid glycosidic lignin ester were also reported as components in the *Olea* genus [8]. Oleanolic acid, a biologically active compound isolated from the chloroform extract of *O. ferruginea* R., was shown to exhibit antitumor, antimicrobial, hepatoprotective, and antiallergic potential [9,10], while neuroprotective effects were observed in a focal brain hypoxia rat model [11]. *Olea europaea* and other species have also potent antiviral activity against several viruses [8]. More in general, the leaves of *Olea* species have been traditionally used in Mediterranean and European regions for treating hypertension, bacterial infections, and hyperglycemia in diabetic patients [12]. Similarly, the *Olea* fruit has been reported to have antihyperglycemic action in cell cultures and animal models [8].

On such basis, the present study aimed at investigating ferruginan from *O. ferruginea* for its in vitro anti-inflammatory and anti-diabetic activity.

2. Results

2.1. Extraction and Characterization of Ferruginan

The ethyl acetate fraction of *O. ferruginea* extract was subjected to normal-phase liquid chromatography, which yielded purified ferruginan (Figure 1). We obtained 1.02 g of compound from 7.00 kg of dried plant material (extraction yield: 1.46×10^{-2}% *w/w*). Ferruginan identity was initially checked by precoated TLC visualized under UV light. The structure of the isolated compound was identified previously by our research group through UV analysis, advanced NMR analysis, and mass spectrometry, and the spectra were in agreement with reported literature data [6]. In particular, the UV spectrum showed maximum absorption at 230 and 283 nm, and the structure of ferruginan was fully supported by 2D-NMR spectral data such as HSQC, HMBC, and COSY spectra, which were closely related to those reported [6,13].

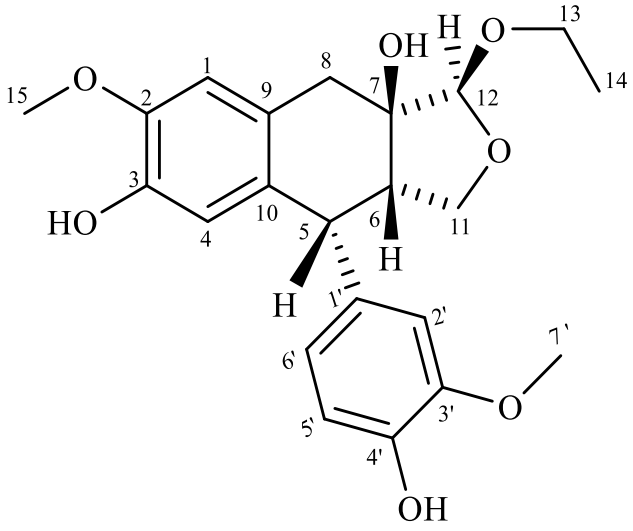

Figure 1. Chemical structure of ferruginan isolated from *O. ferruginea.*

It must be noted that ferruginan was previously investigated as a cytotoxic agent and showed mild cytotoxic activity in MCF-7 cells (IC_{50} = 10.41 µg/mL) [6]. Moreover, our group evaluated ferruginan as a potential leishmanicidal and antioxidant compound [6,13].

In the present study, the anti-inflammatory and anti-diabetic actions of ferruginan isolated from *O. ferruginea* were investigated using in vitro models, and such studies were paralleled by preliminary computational simulations.

2.2. In Vitro Anti-Inflammatory Activity

The role of ferruginan on membrane stabilization was evaluated by measuring the inhibition of the lysis of human red blood cells' (HRBCs) membrane at high temperature. This method is adopted to evaluate the anti-inflammatory effect of a molecule. The hemoglobin level in the samples was measured, and the experiment showed that ferruginan inhibited inflammation. For comparison, the standard drug diclofenac sodium was used as a reference in the experiment. Various concentrations of the compound were used, i.e., 10, 20, 30, 40, 50, 80, and 100 µM, which showed 10.96%, 21.89%, 38.74%, 50.61%, 59.75%, 65.91%, and 71.82% of inhibition, respectively. An IC_{50} value of 53.91 µM was calculated for ferruginan. Concerning the positive control, diclofenac sodium was used at 10, 20, 30, 40, 50, 80, and 100 µM concentrations, which showed 32.66%, 64.23%, 73.80%, 77.38%, 78.57%, 80.95%, and 85.71% of inhibition, respectively. Figure 2 shows the results of the test, demonstrating that the activity of ferruginan paralleled that of the standard. The minimum rate of inhibition for ferruginan was measured at 10 µM (10.96%), while the maximum rate of inhibition was shown at 100 µM and was 71.82%.

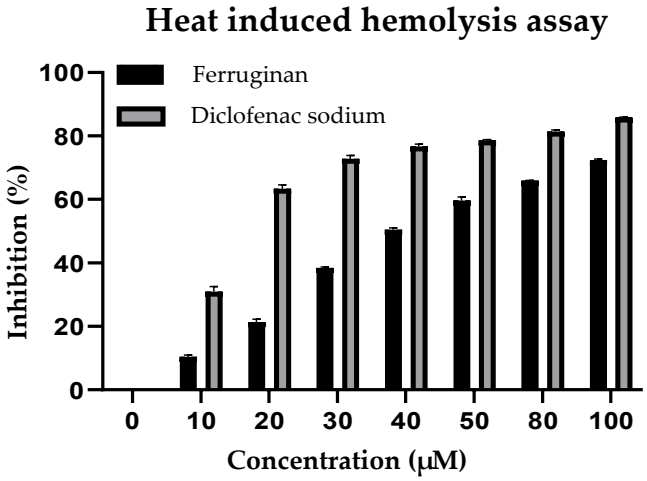

Figure 2. Effect of ferruginan, in comparison with diclofenac sodium (standard), in the heat-induced hemolysis assay. Experiments were performed in triplicate, and values are reported as mean ± SD.

2.3. In Vitro Anti-Diabetic Activity

To study the effects of ferruginan on glucose uptake in yeast cells in a 5 mM glucose solution, various concentrations of the compound (from 5 µM to 100 µM) were tested. Impaired glucose uptake by cells is one of the hallmarks of diabetes, and insulin-sensitizing antihyperglycemic agents act by facilitating the action of insulin in promoting glucose distribution. The studied compound increased glucose uptake from 6.71% to 74.96% in yeast cells at 5 µM and 100 µM, respectively, showing an EC_{50} value of 47.12 µM and indicating that the observed effect was dose-dependent. The standard drug metronidazole has also a pronounced effect on glucose uptake by yeast cells. According to the assay, there was an increase from 17.09% and 85.71% in glucose uptake at 5 µM and 100 µM of metronidazole, respectively. The results of the test are reported in Figure 3, which shows that the activity of the tested compound paralleled that of the standard.

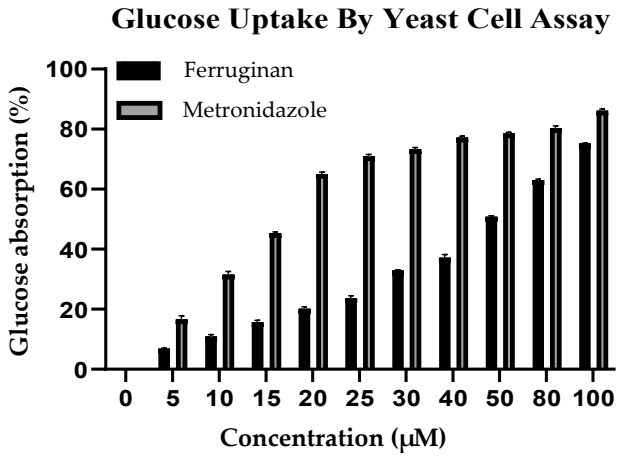

Figure 3. Results of the glucose yeast uptake assay (5 mM glucose) for ferruginan and metronidazole (standard). Experiments were performed in triplicate, and values are reported as mean ± SD.

2.4. α-Amylase Inhibition Assay

Noteworthy results were produced by ferruginan also in the α-amylase inhibition assay. More specifically, the activity of the compound was determined at increasing concentrations, i.e., 10, 20, 40, 60, 80, and 100 μM, for which the recorded inhibition percentage was 12.51%, 15.32%, 31.90%, 50.12%, 67.68%, and 75.45%, respectively. The compound expressed an IC_{50} value of 43.47 μM. Acarbose was used as a reference and, at 100 μM, inhibited the enzyme activity by 87.85%. The results of dose-dependent enzyme inhibition are reported in Figure 4, together with a representative model of the interaction of acarbose and ferruginan with the protein.

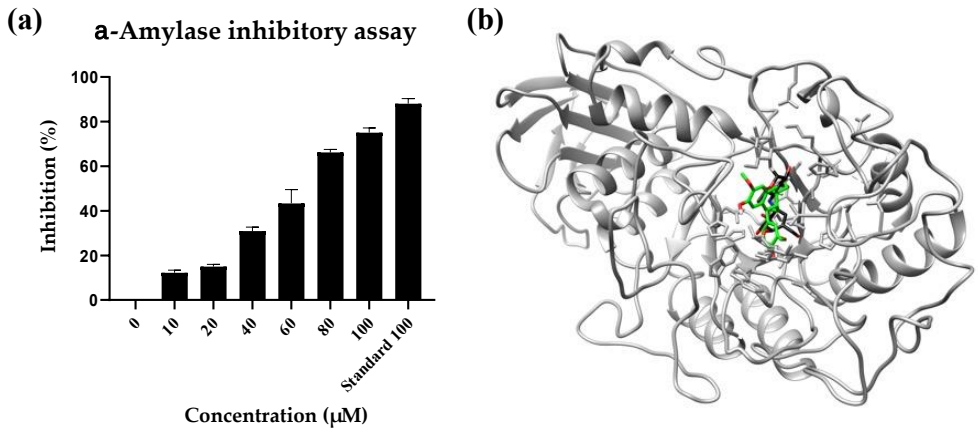

Figure 4. Effect of ferruginan on α-amylase activity at various concentrations. Acarbose was used as a standard; the experiments were performed in triplicate, and the values are reported as mean ± SD (**a**). Representative model showing the interaction of ferruginan (green, docked pose −7.6 kcal/mol), in comparison with co-crystallized acarbose (black), with α-amylase (1B2Y, artwork produced with UCSF Chimera) (**b**).

2.5. Molecular Docking towards Targets Involved in Inflammation

In the subsequent step of this study, we aimed at exploring the mechanism(s) of action through which ferruginan may exert the observed biological effects, by means of computational tools.

Target pathway prediction tools were utilized to hypothesize the involved molecular mechanisms. According to the ligand-based study carried out using PathwayMap [14], ferruginan was predicted to target several pathways. Nevertheless, the five mechanisms

for a which a higher score was computed were "signal transduction" (in particular, cAMP pathway, score 0.174), "endocrine system" (in particular, insulin secretion, score 0.158), "cell proliferation" (score 0.135), "amino acid metabolism" (in particular, lysine degradation, score 0.121), and "cardiovascular disease" (score 0.101).

Then, in our preliminary docking study, we considered four molecular targets known to be involved mainly in inflammation but also in diabetes to perform the docking studies. More in detail, 5′-adenosine monophosphate-activated protein kinase (AMPK), cyclooxygenase-1 (COX-1), cyclooxygenase-2 (COX-2), and tumor necrosis factor alpha (TNF-α) were thus selected. The tree-dimensional (3D) crystal structures of all the target macromolecules were obtained from the Protein Data Bank (PDB). The PDB codes of the downloaded enzymes are the following: 3AQV (for AMPK), 1EQG (For COX-1), 1CX2 (COX-2), and 2AZ5 (for TNF-α) [15–18]. After the preparation of the downloaded models, their native ligands were redocked into the binding pockets of their respective proteins to validate the docking protocols, and procedures leading to RMSD values lower than 2.0 Å were used for further studies.

The docking simulations showed that in the binding site of AMPK, the native ligand interacts with Val96 via hydrogen bond interactions, while Tyr95 (π-π stack) and Met93 (π-sulfur) form hydrophobic interactions. Ferruginan forms three hydrogen bonds with Val96, Glu100, and Asp103, while Tyr95 establishes π–π stacking as a hydrophobic interaction. The binding energy value computed for ferruginan was −7.67 kcal/mol. Overall, the two compounds establish a similar interaction pattern with the target and bind to the same region of the protein, as depicted in Figure 5.

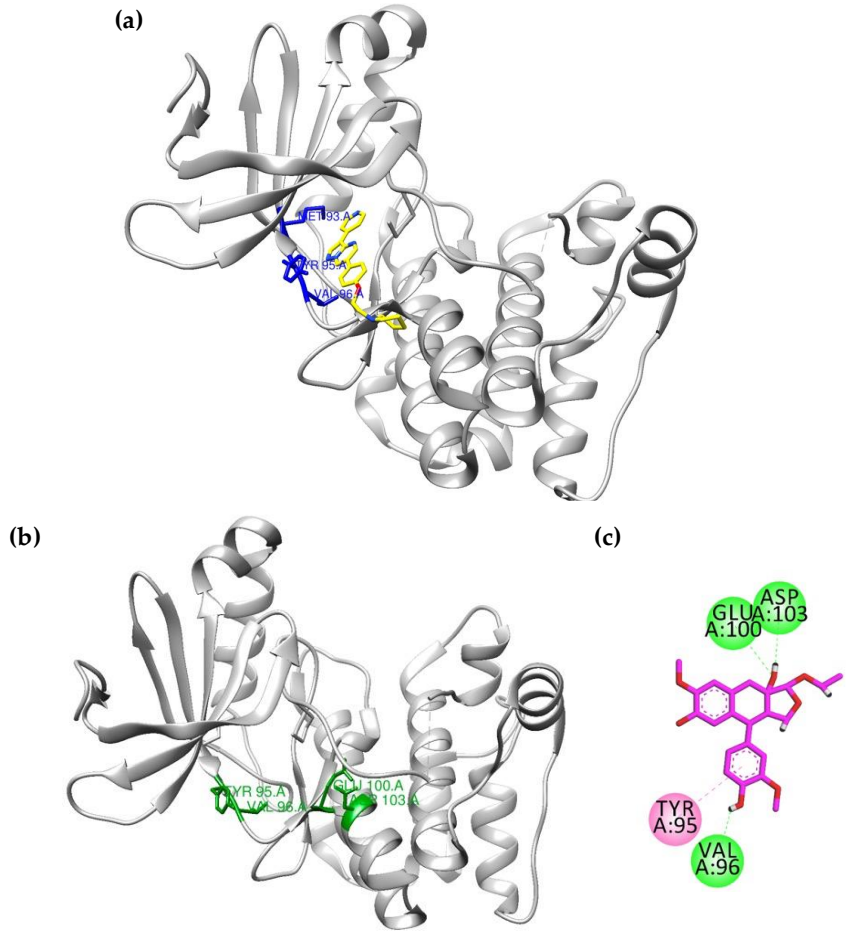

Figure 5. Predicted interaction pattern, in terms of involved residues, for (**a**) the native ligand and (**b**) ferruginan in the binding site of AMPK. The involved residues are highlighted, and the amino acids targeted by ferruginan are also reported in panel (**c**).

For investigating its role in the context of the inflammatory response, ferruginan was also docked into the binding sites of COX-1 and COX-2. In the binding site of COX-1, hydrogen bond interactions with Leu352 were highlighted, while Val349, Ile523, and Ala52 appeared to interact via π–σ interactions (Figure 6a). In the binding site of COX-2, the hydroxyl group appeared oriented towards the COX-2 specific pocket and to form hydrogen bond interactions with His90 and Ser353. A weak π–alkyl interaction was also observed between the phenyl ring and Val523, an important residue of this pocket. Tyr385 was also shown to interact with the compound via a hydrogen bond (Figure 6b). The computed binding energy values in the binding site of COX-1 and COX-2 were −4.81 kcal/mol and −7.36 kcal/mol, respectively. Eventually, in the binding site of TNF-α, ferruginan was found to interact with amino acid residues via hydrogen bond interactions. The residues involved in the interaction were identified as Ser60, Gly121, and Tyr151 (Figure 6c). The computed binding energy value for ferruginan in this site corresponded to −6.16 kcal/mol.

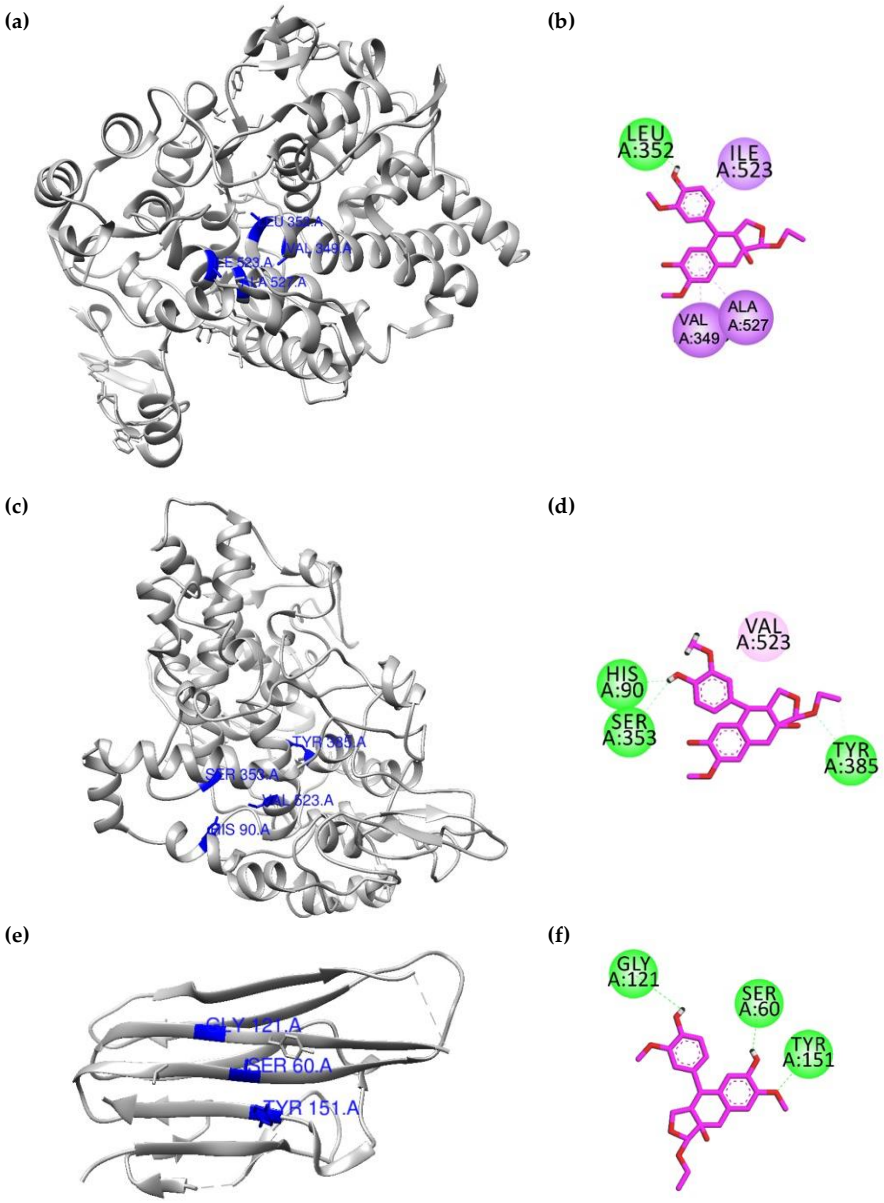

Figure 6. Predicted interaction pattern, in terms of involved residues, for ferruginan with COX-1 (**a**,**b**), COX-2 (**c**,**d**), and TNF-α (**e**,**f**). The targeted amino acids are highlighted, and 2D interaction maps are reported.

3. Discussion

O. ferruginea is a medicinal plant traditionally used to treat different diseases and conditions such as teeth problems, fever, skeleton disorders, debility, and even cancer cell proliferation [10]. Its bark possesses antidiabetic and cytotoxic potential. It has also been reported as a possible tool to treat asthma, rheumatism, wounds, and malaria, and its dried fruits are used for lowering the blood glucose level [19].

Inflammation is a complex response of the body that acts against various damages in cells, tissues, and organs caused by stimuli such as mechanical injuries, allergens, burns, microbial infections, and other toxic substances which activate macrophages, leukocytes, mast cells, and complement factors [20]. Diabetes is related to inflammation, and the treatment of DM in the current scenario is mainly based on parenteral insulin and oral anti-diabetic drugs. Due to the serious side effects of oral hypoglycemic agents, there is a need to search newer anti-diabetic agents having minimum side effects and high therapeutic efficacy [21]. In Pakistan, medicinal plants are mostly used locally by the rural population, since the soil is rich in this natural resource, especially in northern areas, where lush green mountains still host unidentified wild plants. It is of primary relevance to gain a deep knowledge concerning herbs and their constituents, especially considering their therapeutic activity and potential synergistic effects with other drugs [22].

Ferruginan is a compound that, according to its physico-chemical properties calculated using SwissADME, can be defined as drug-like. This molecule is predicted to be moderately soluble in water. As reported in Supplementary Information, ferruginan falls within the ideal chemical space in terms of lipophilicity, size, polarity, solubility, degree of instauration, and flexibility for a drug-like compound (Figure S1) [23].

The effect of ferruginan from *O. ferruginea* on HRBC membrane stabilization was tested by measuring the hemoglobin level in the samples after inhibiting HRBC membrane hemolysis at high temperatures. Ferruginan counteracted inflammation by reducing the hemolysis of HRBCs at high temperature dose-dependently. For comparison, diclofenac sodium was used as a standard drug [24]. The maximum degree of inhibition for ferruginan was reached at 100 μM (71.82%).

Then, to study the effect of the compound on glucose uptake by yeast cells in a 5 mmol glucose solution, various concentrations of the isolated molecule (from 5 μM to 100 μM) were tested. In fact, the utilization of carbohydrates is greatly affected by DM, which leads to an imbalance in the metabolism of lipids [25]. The compound dose-dependently increased the uptake of glucose to a maximum of 74.96% at 100 μM. The standard drug metronidazole, which was used as a reference, had an even more marked effect on glucose uptake, leading to an increase of up to 85.71% in yeast cells at a 100 μM concentration.

Moreover, ferruginan inhibited α-amylase, an enzyme that breaks polysaccharides to produce glucose and maltose, dose-dependently and by up to 75.45% at 100 μM, in a range similar to that of the control compound acarbose. This evidence further supports the potential role of ferruginan as an anti-diabetic agent.

Then, we performed ligand-based target prediction studies which highlighted that inflammation and glucose degradation pathways may indeed be involved in the activity of ferruginan. Moreover, preliminary docking data showed that ferruginan binds to the same pocket occupied by acarbose in the enzyme.

In general, the causes and risk factors of diabetes are genetic and environmental conditions. The deregulation of the immunological and inflammatory systems increases the vulnerability to type 1 and type 2 diabetes, according to evidence from the past 10 years. On this basis, by means of computational tools, we explored the mechanism of action of ferruginan isolated from *O. ferruginea*. For this purpose, we selected four molecular targets for the docking studies. AMPK is considered a key target to design drugs against obesity, metabolic syndrome, and type 2 diabetes. Detailed views of the predicted interaction patterns of ferruginan with the studied targets are reported in Supplementary Information (Figures S2–S5).

These computational studies carried out on various macromolecular targets involved in the abovementioned diseases suggested that ferruginan may preferentially act through the interaction with COX-2 and AMPK, for which the most promising calculated binding values were retrieved. More specifically, the docking scores computed for ferruginan were overall not optimal. Nevertheless, it must be considered that the compound indeed showed the higher number of hydrogen bonds with these two proteins compared to other targets (Figures 5 and 6).

4. Materials and Methods

4.1. Plant Collection and Processing

The aerial parts of *O. ferruginea* Royle plants were collected from the Agriculture Research Institute Tarnab, Peshawar, Khyber Pakhtunkhwa, Pakistan, in the month of May, and the samples were identified by Dr. Muhammad Ilyas at the Department of Botany, University of Swabi. The plant was washed with tap water to remove any dust particles and then was shade-dried. The dried plant material (7.00 kg) was finally grinded to powder and stored for further processing.

4.2. Extraction and Isolation

For the crude methanolic extract preparation, *O. ferruginea* powder (7.00 kg) was suspended in methanol and kept for 7 days at room temperature with occasional mixing and shaking. After that, all insoluble components were filtered. The filtrate was evaporated through a rotary evaporator at 45 °C to obtain a semi-solid crude extract (87.00 g). Then, 22.54 g of the extract was dissolved in ethyl acetate and then subjected to further purification. More in detail, silica gel column chromatography was performed after dry loading of the sample by using hexane and ethyl acetate (75:25) as a mobile phase, affording ferruginan as an isolated compound (1.02 g). The analytical profile of the extracted compound was in agreement with data reported previously [6,13].

4.3. In Vitro Anti-Inflammatory Activity

The in vitro anti-inflammatory activity assay was performed to evaluate the heat-induced hemolysis activity. This test examines the stabilization and lysis of the plasma membrane of red blood cells. The assay was carried out by the method reported in [24], with minor modifications. The potency of the compound was tested at high temperature, measuring the inhibition of RBC membrane lysis through the assay. The experimental protocol was approved by the Research grants and Experimentation Ethics Committee of the Department of Zoology, Abdul Wali Khan University, Mardan, on the use of human tissue samples and blood. Fresh blood was collected from healthy volunteers in EDTA tubes and centrifuged at 3000 rpm for 15 min. The supernatant was discarded, while the pellet was washed with an isosaline solution. The process was repeated 3 times until a clear supernatant appeared. The pellet containing human red blood cells (HRBCs) was used to prepare a 10% suspension in an isotonic saline solution. Diclofenac sodium in phosphate-buffered saline (PBS, pH 7.4) was used as a control in this test. The control reaction mixture contained 100 µL of the 10% blood suspension, 20 µL of distilled water, and 880 µL of PBS solution. The standard reaction mixture contained 100 µL of the 10% blood suspension and various concentrations of diclofenac sodium (DS) in PBS solution (10 µg DS + 890 µL PBS, 20 µg DS + 880 µL PBS, 30 µg DS + 870 µL PBS, and 80 µg DS + 820 µL PBS). The test sample reaction mixture contained 100 µL of the 10% blood suspension and various concentrations of the compound in PBS solution (10 µM compound + 890 µL PBS, 20 µM compound + 880 µL PBS, 30 µM compound +870 µL PBS, and 80 µM compound + 820 µL PBS). Incubation was performed at 54 °C for 30 min, then the samples were centrifuged at 5400 rpm for 5 min. All samples were analyzed in triplicate, and absorbance was analyzed

through a spectrophotometer (UV5100B, PIOWAY, Nanjing, China) at 560 nm. The formula used for the determination of the percentage of inhibition of HRBC lysis is reported below:

$$\%\text{inhibition} = \frac{\text{Abs(control)} - \text{Abs(sample)} \times 100}{\text{Abs(control)}} \quad (1)$$

All the tests were performed in triplicate, and the mean ± SD was calculated.

4.4. In Vitro Anti-Diabetic Activity

The in vitro anti-diabetic activity was tested by determining the glucose uptake using the yeast cells assay. The assay was performed as per the method described in [17] with slight modifications. Yeast cells have affinity for glucose uptake and thus they are used as a model for diabetes. Baker's yeast was washed by repeated centrifugation in distilled water till the appearance of a clear supernatant. Then, a 10% colloidal suspension from the pellet was added to distilled water. Different concentrations of the compound were incubated with 1 mL of the solution containing glucose (5 mM). All samples were incubated at 37 °C for 10 min, and then the yeast suspension was added to start the reaction. The samples were vortexed and incubated further for 1 h at 37 °C, then they were finally centrifuged at 3000 rpm for 5 min. The amount of glucose uptake was determined through a spectrophotometer (UV5100B, PIOWAY, China) at 520 nm. The percentage increase in glucose uptake in the yeast cells was measured using Formula (1). All the tests were performed in triplicate, and the mean ± SD was calculated.

4.5. α-Amylase Inhibition Assay

Different concentrations of the compound and the reference standard drug were incubated with 2 U/mL of porcine pancreatic amylase (500 µL) in phosphate buffer for 20 min at 37 °C. Then, 250 µL of 1% starch was added, and the reaction was incubated for 1 h at 37 °C. Afterwards, 1 mL of dinitro salicylate reagent was added, and the mixture was boiled for 10 min. The absorbance was then measured at 540 nm, and the values were compared to those obtained for the control to calculate the inhibitory activity. Formula (1) was used for the calculations. All the tests were performed in triplicate, and the mean ± SD was calculated.

4.6. Molecular Modeling

The physico-chemical parameters were computed using SwissADME [23], and the target prediction studies were performed using PathwayMap [14].

For the docking studies, the 3D crystal structures of all the target macromolecules were obtained from PDB (https://www.rcsb.org/ accessed on 23 December 2022). The PDB codes of the downloaded enzymes are: 3AQV (AMPK), 1EQG (COX-1), 1CX2 (COX-2), and 2AZ5 (TNF-α). For α-amylase, shown in Figure 4, the 1B2Y model was used. The ligand and downloaded targets were prepared by using previously reported procedures [18,19]. The docking studies were carried out by using Molecular Operating Environment (MOE 2016.0802). The downloaded proteins were prepared and 3D protonated by using the "Prepare" module of MOE. Energy minimization was carried out by using AMBER 10EHT forcefield. For the docking simulations, docking grids were determined within 10 Å from the co-crystallized ligands. For all the ligands, 10 conformations were generated, and the top-ranked conformations based on the docking score were selected. Ligand interaction and visualization were carried out via Discovery Studio Visualizer (BIOVIA, Dassault Systèmes, San Diego, CA, USA) and UCSF Chimera, which were also used for the analysis of the docking results [26].

5. Conclusions

The present study on ferruginan extracted from *O. ferruginea* demonstrates that this natural compound has anti-inflammatory and anti-diabetic multi-target potential, as proved by a set of in vitro assays, including the α-amylase inhibition test, supported by computa-

tional data. Ligand-based target prediction and preliminary docking studies suggest that ferruginan may act on various molecular targets involved in diabetes and inflammation. On the other hand, it must be observed that the compound showed promising bioactivity, according to the tests performed on inflammation, glucose uptake, and α-amylase inhibition, only at rather high concentrations. This suggests that optimization of the small molecule is mandatory, as higher potency is needed for a future development as a drug candidate. Moreover, it must be stressed that while this study paved the way for the investigation of the bioactivity of ferruginan through computational and experimental evidence, further in vitro and in vivo studies are needed to fully assess the pharmacological potential and safety of this natural compound.

Supplementary Materials: The following supporting information can be downloaded at: https://www.mdpi.com/article/10.3390/pr11020545/s1, Figures S1–S5: computational studies and interaction pattern of native ligands and docked compounds.

Author Contributions: Conceptualization, A.R. (Abdur Rauf) and U.R.; methodology, Z.A.S. and I.; software, G.R. (Giovanni Ribaudo); validation, K.B., J.J., and A.R. (Abdur Rahman); formal analysis, A.A.; investigation, M.A., A.A.-S.; resources, A.A.; data curation, G.R. (Gauhar Rehman); writing—original draft preparation, A.R. (Abdur Rauf), A.A.-S.; writing—review and editing, G.R. (Giovanni Ribaudo); visualization, M.A.; supervision, A.R. (Abdur Rauf); project administration, A.A.; funding acquisition, M.A. All authors have read and agreed to the published version of the manuscript.

Funding: This research was founded by Researchers Supporting Project number (RSP2023R491), King Saud University, Riyadh, Saudi Arabia.

Institutional Review Board Statement: The experimental protocol was approved by the Research grants and Experimentation Ethics Committee of the Department of Zoology Abdul Wali Khan University, Mardan, on the use of human tissue samples and blood (AWKUM/Zoo/2022/2788).

Informed Consent Statement: Not applicable.

Data Availability Statement: The data associated with this paper are provided in the main text of this paper.

Acknowledgments: G.R. acknowledges funding from the University of Brescia.

Conflicts of Interest: The authors declare no conflict to interest.

References

1. Johannsen, D.L.; Ravussin, E. The Role of Mitochondria in Health and Disease. *Curr. Opin. Pharmacol.* **2009**, *9*, 780–786. [CrossRef] [PubMed]
2. Diniz do Nascimento, L.; De Moraes, A.A.B.; Da Costa, K.S.; Galúcio, J.M.P.; Taube, P.S.; Costa, C.M.L.; Cruz, J.N.; Andrade, E.H.D.A.; De Faria, L.J.G. Bioactive Natural Compounds and Antioxidant Activity of Essential Oils from Spice Plants: New Findings and Potential Applications. *Biomolecules* **2020**, *10*, 988. [CrossRef] [PubMed]
3. Rana, A.; Samtiya, M.; Dhewa, T.; Mishra, V.; Aluko, R.E. Health Benefits of Polyphenols: A Concise Review. *J. Food Biochem.* **2022**, *46*, e14264. [CrossRef] [PubMed]
4. Atanasov, A.G.; Zotchev, S.B.; Dirsch, V.M.; Supuran, C.T. Natural products in drug discovery: Advances and opportunities. *Nat. Rev. Drug Discov.* **2021**, *20*, 200–216. [CrossRef]
5. Sarker, S.D.; Nahar, L. An Introduction to Natural Products Isolation. *Methods Mol. Biol.* **2012**, *864*, 1–25. [CrossRef]
6. Shah, Z.A.; Mujawah, A.A.H.; Ullah, I.; Rauf, A.; Rashid, U.; Khalil, A.A.; Shah, S.M.M.; Pervaiz, A.; Shaheen, F.; Al-Awthan, Y.S.; et al. Antioxidant and Cytotoxic Activity of a New Ferruginan A from Olea Ferruginea: In Vitro and In Silico Studies. *Oxidative Med. Cell. Longev.* **2022**, *2022*, 8519250. [CrossRef]
7. Amin, A.; Khan, M.A.; Shah, S.; Ahmad, M.; Zafar, M.; Hameed, A. Inhibitory Effects of Olea Ferruginea Crude Leaves Extract against Some Bacterial and Fungal Pathogen. *Pak. J. Pharm. Sci.* **2013**, *26*, 251–254.
8. Anwar, S.; Saleem, H.; Khurshid, U.; Ansari, S.Y.; Alghamdi, S.; Al-Khulaidi, A.W.A.; Malik, J.A.; Ahemad, N.; Awadh Ali, N.A. Comparative Phytochemical Composition, Oleuropein Quantification, Antioxidant and Cytotoxic Properties of *Olea Europaea* L. Leaves. *Nat. Prod. Res.* **2022**, 1–7. [CrossRef]
9. Ayeleso, T.; Matumba, M.; Mukwevho, E. Oleanolic Acid and Its Derivatives: Biological Activities and Therapeutic Potential in Chronic Diseases. *Molecules* **2017**, *22*, 1915. [CrossRef]
10. Mehmood, A.; Murtaza, G. Phenolic Contents, Antimicrobial and Antioxidant Activity of Olea Ferruginea Royle (Oleaceae). *BMC Complement. Altern. Med.* **2018**, *18*, 173. [CrossRef]

11. Sun, N.; Li, D.; Chen, X.; Wu, P.; Lu, Y.-J.; Hou, N.; Chen, W.-H.; Wong, W.-L. New Applications of Oleanolic Acid and Its Derivatives as Cardioprotective Agents: A Review of Their Therapeutic Perspectives. *Curr. Pharm. Des.* **2019**, *25*, 3740–3750. [CrossRef] [PubMed]
12. Yu, M.; Gouvinhas, I.; Rocha, J.; Barros, A.I.R.N.A. Phytochemical and Antioxidant Analysis of Medicinal and Food Plants towards Bioactive Food and Pharmaceutical Resources. *Sci. Rep.* **2021**, *11*, 10041. [CrossRef]
13. Zafar, S.; -Ur-Rehman, F.; Shah, Z.A.; Rauf, A.; Khan, A.; Humayun Khan, M.; Ur Rahman, K.; Khan, S.; Ullah, A.; Shaheen, F. Potent Leishmanicidal and Antibacterial Metabolites from *Olea Ferruginea*. *J. Asian Nat. Prod. Res.* **2019**, *21*, 679–687. [CrossRef] [PubMed]
14. Jiménez, J.; Sabbadin, D.; Cuzzolin, A.; Martínez-Rosell, G.; Gora, J.; Manchester, J.; Duca, J.; De Fabritiis, G. PathwayMap: Molecular Pathway Association with Self-Normalizing Neural Networks. *J. Chem. Inf. Model.* **2019**, *59*, 1172–1181. [CrossRef] [PubMed]
15. He, M.M.; Smith, A.S.; Oslob, J.D.; Flanagan, W.M.; Braisted, A.C.; Whitty, A.; Cancilla, M.T.; Wang, J.; Lugovskoy, A.A.; Yoburn, J.C.; et al. Small-Molecule Inhibition of TNF-α. *Science* **2005**, *310*, 1022–1025. [CrossRef]
16. Kurumbail, R.G.; Stevens, A.M.; Gierse, J.K.; McDonald, J.J.; Stegeman, R.A.; Pak, J.Y.; Gildehaus, D.; Iyashiro, J.M.; Penning, T.D.; Seibert, K.; et al. Structural Basis for Selective Inhibition of Cyclooxygenase-2 by Anti-Inflammatory Agents. *Nature* **1996**, *384*, 644–648. [CrossRef]
17. Selinsky, B.S.; Gupta, K.; Sharkey, C.T.; Loll, P.J. Structural Analysis of NSAID Binding by Prostaglandin H $_2$ Synthase: Time-Dependent and Time-Independent Inhibitors Elicit Identical Enzyme Conformations. *Biochemistry* **2001**, *40*, 5172–5180. [CrossRef]
18. Handa, N.; Takagi, T.; Saijo, S.; Kishishita, S.; Takaya, D.; Toyama, M.; Terada, T.; Shirouzu, M.; Suzuki, A.; Lee, S.; et al. Structural Basis for Compound C Inhibition of the Human AMP-Activated Protein Kinase A2 Subunit Kinase Domain. *Acta Cryst. D Biol. Crystallogr.* **2011**, *67*, 480–487. [CrossRef]
19. Liaqat, S.; Islam, M.; Saeed, H.; Iqtedar, M.; Mehmood, A. Investigation of Olea Ferruginea Roylebark Extracts for Potential in Vitro Antidiabetic and Anticancer Effects. *Turk. J. Chem.* **2021**, *45*, 92–103. [CrossRef]
20. Shams, W.A.; Rehman, G.; Onoja, S.O.; Ali, A.; Khan, K.; Niaz, S. In Vitro Antidiabetic, Anti-Inflammatory and Antioxidant Potential of the Ethanol Extract of Uromastyx Hardwickii Skin. *Trop. J. Pharm. Res.* **2021**, *18*, 2109–2115. [CrossRef]
21. Sagbo, I.J.; van de Venter, M.; Koekemoer, T.; Bradley, G. In Vitro Antidiabetic Activity and Mechanism of Action of *Brachylaena Elliptica* (Thunb.) DC. *Evid.-Based Complement. Altern. Med.* **2018**, *2018*, 4170372. [CrossRef] [PubMed]
22. Sekhon-Loodu, S.; Rupasinghe, H.P.V. Evaluation of Antioxidant, Antidiabetic and Antiobesity Potential of Selected Traditional Medicinal Plants. *Front. Nutr.* **2019**, *6*, 53. [CrossRef] [PubMed]
23. Daina, A.; Michielin, O.; Zoete, V. SwissADME: A Free Web Tool to Evaluate Pharmacokinetics, Drug-Likeness and Medicinal Chemistry Friendliness of Small Molecules. *Sci. Rep.* **2017**, *7*, 42717. [CrossRef] [PubMed]
24. Rehman, G.; Hamayun, M.; Iqbal, A.; Ul Islam, S.; Arshad, S.; Zaman, K.; Ahmad, A.; Shehzad, A.; Hussain, A.; Lee, I. In Vitro Antidiabetic Effects and Antioxidant Potential of *Cassia nemophila* Pods. *BioMed Res. Int.* **2018**, *2018*, 1824790. [CrossRef]
25. Diedisheim, M.; Carcarino, E.; Vandiedonck, C.; Roussel, R.; Gautier, J.-F.; Venteclef, N. Regulation of Inflammation in Diabetes: From Genetics to Epigenomics Evidence. *Mol. Metab.* **2020**, *41*, 101041. [CrossRef]
26. Pettersen, E.F.; Goddard, T.D.; Huang, C.C.; Couch, G.S.; Greenblatt, D.M.; Meng, E.C.; Ferrin, T.E. UCSF Chimera?A Visualization System for Exploratory Research and Analysis. *J. Comput. Chem.* **2004**, *25*, 1605–1612. [CrossRef]

Disclaimer/Publisher's Note: The statements, opinions and data contained in all publications are solely those of the individual author(s) and contributor(s) and not of MDPI and/or the editor(s). MDPI and/or the editor(s) disclaim responsibility for any injury to people or property resulting from any ideas, methods, instructions or products referred to in the content.